

Evaluating DNA function understanding in genomic language models using evolutionarily implausible sequences

Shiyu Jiang^{1,2,*}, Xuyin Liu¹, and Zitong Jerry Wang^{1,*}

¹Center for Interdisciplinary Studies, School of Science, Westlake University, Hangzhou, China

²Department of Quantitative and Computational Biology, University of Southern California, Los Angeles, CA, United States

*Correspondence to shiyujia@usc.edu and jerry@westlake.edu.cn

Abstract

Genomic language models (gLMs) hold promise for generating novel, functional DNA sequences for synthetic biology. However, realizing this potential requires models to go beyond evolutionary plausibility and understand how DNA sequence encodes gene expression and regulation. We introduce a benchmark called Nullsettes, which assesses how well models can predict *in silico* loss-of-function (LOF) mutations, in synthetic expression cassettes with little evolutionary precedent. Testing 12 state-of-the-art gLMs, we find that most fail to consistently detect these strong LOF mutations. All models show a sharp drop in predictive accuracy as the likelihood assigned to the original (nonmutant) sequence decreases, suggesting that gLMs rely heavily on pattern-matching to their evolutionary prior rather than on any mechanistic understanding of gene expression. Our findings highlight fundamental limitations in how gLMs generalize to engineered, non-natural sequences, and underscore the need for benchmarks and modeling strategies that prioritize functional understanding.

Keywords: genomic language model, synthetic biology, mutation prediction, gene expression, regulatory genomics

1 Background

Genomic language models (gLMs) learn a probability distribution over naturally occurring DNA sequences, approximating the evolutionary plausibility of a sequence or its probability of arising and persisting under evolutionary constraints [1, 2]. This plausibility reflects factors such as the presence of common regulatory motifs or similarity to known natural genomes. For example, gLMs tend to assign higher likelihoods to promoters with frequent natural motifs than to random synthetic promoters.

Evolutionary plausibility can be a useful proxy for biological function, as gLMs have already demonstrated strong zero-shot performance in predicting mutation effects to support sequence design. In both genomic and protein language models (gLMs and pLMs), higher model likelihoods often correlate with improved functional properties. For example, pLM likelihoods can guide the design of higher antibodies [3], more efficient base editors [4], brighter fluorescent proteins [5], and deep mutational scanning (DMS) tasks [6, 7]. Similarly, gLM likelihoods enable genome-wide prediction of variant effects [8] and 5' untranslated region (UTR) optimization [9].

However, it remains unclear whether gLMs trained solely on natural genomes understand DNA function well enough to generalize to synthetic constructs with little to no evolutionary precedent. Current evaluations for gLMs on mutation effect prediction focus primarily on natural sequences, such as variants within endogenous cis-regulatory elements and splice sites [10]. In contrast, synthetic biology often requires the design of functional sequences with little evolutionary history, to solve industrial challenges, avoid crosstalk with native pathways, or push expression levels beyond natural limits. Examples include ultra-strong synthetic promoters [11], miRNA-based regulatory circuits that achieve dosage-compensated gene expression using elements orthogonal to native miRNAs [12], and engineered metabolic pathways for production of small molecule drugs [13]. We need evaluation benchmarks that test whether models can generalize beyond evolutionary patterns to capture functional principles to help rewire biology.

Fundamental mechanisms of gene expression are conserved across all domains of life, making it an ideal test of functional understanding. We introduce, Nullsettes, a benchmark for evaluating whether gLMs can predict loss-of-function (LOF) mutations in synthetic expression cassettes. We create these LOF mutations *in silico* by rearranging key regulatory elements, such as promoters and start codons, within nonmutant cassettes. These rearrangements disrupt the canonical sequence structure required for transcription and translation, rendering the sequences non-functional. We curate nonmutant cassettes from massive parallel reporter assay (MPRA) datasets [14, 15, 16, 17]. GLMs assign low likelihood to these cassette as they contain genetic elements from evolutionarily distant species, and incorporate random sequences functioning as promoters.

Across 12 state-of-the-art models (and 28 variants) spanning a wide range of design choices, we find that gLMs perform poorly on zero-shot LOF prediction, particularly under contexts that deviate strongly from natural sequence statistics. For example, model performance worsens when mutations cause more severe functional disruption, or when cassettes include strong promoters drawn from random sequence libraries. Notably, all models show a sharp drop in prediction accuracy as the likelihood of the nonmutant sequence decreases, indicating that gLMs rely heavily on pattern-matching to their evolutionary priors rather than on functional understanding of gene expression. Accurate predictions only emerge when the nonmutant likelihood surpasses a length-scaled threshold. Comparisons between models show that functional general-

ization may depend more on the relevance and quality of pretraining data than on the sheer size of the dataset. These findings highlight fundamental limitations in how current gLMs generalize to engineered sequences, and underscore the need for benchmarks and modeling strategies that prioritize the functional understanding of DNA sequences.

2 Results and discussion

We design Nullsettes as a benchmark to test whether genomic language models (gLMs) understand functional gene expression in sequences that lack evolutionary plausibility. Nullsettes consists of zero-shot mutation effect prediction tasks, where synthetic expression cassettes are subjected to virtual loss-of-function (LOF) mutations created by rearranging key genetic elements.

In a canonical eukaryotic expression cassette (Figure 1A, i–ii), control elements including the promoter, start codon, coding sequence (CDS), stop codon, and terminator must appear in a specific 5'-3' order to enable proper transcription and translation. Rearranging these elements, for example, placing a terminator upstream of the CDS (iii) or positioning the CDS downstream of the stop codon (iv), disrupts this structure and results in nonfunctional gene expression. Nullsettes focuses on single-element translocations that eliminate functional protein expression and cannot be rescued by any upstream or downstream sequences (Figure 1B). From these criteria, we obtain 11 mutation types for eukaryotic and 19 for prokaryotic cassettes, with additional prokaryotic variants involving rearrangement of ribosome binding site (RBS) (Supplementary Table S1, S2).

To ensure these tasks test generalization beyond evolutionary prior, we generate virtual mutants from synthetic expression cassettes with low gLM-assigned likelihoods but strong gene expression in either *E. coli*, yeast, or human, drawn from five massively parallel reporter assay (MPRA) datasets [14, 15, 16, 17] (Figure 1B). These cassettes combine sequences from distantly related species, for example, GFP as CDS from *Aequorea victoria* with promoters and terminators from bacteria, human, or mouse. Many cassettes even use random (but functional) promoters, which further lower gLM-assigned likelihood (Supplementary Figure S1). Together, these cassettes enable evaluation of model generalization to functional yet evolutionarily implausible sequences across species.

Given all cassettes in a dataset, we evaluate mutation effect prediction in a zero-shot setting by comparing the distribution of nonmutant log-likelihood (LL) to the distribution of corresponding Nullsettes mutants (Figure 1B). We consider a model capable of identifying a mutation type if the mutant LL are significantly lower than the nonmutant LL, as determined by a paired t-test. A model's success rate on the dataset is the proportion of mutation types identified.

Across five datasets, we found that most genomic language models perform poorly in predicting LOF mutants in Nullsettes. We evaluated 12 representative models (and 28 variants; Supplementary Table S3, S4, and S5) spanning state-of-the-art approaches to genomic language modeling. Nine out of twelve models achieved < 50% success rate on at least one dataset, failing to identify strong LOF mutations (Figure 1C). Only Evo2-7B and GENERanno-0.5B deliver strong, consistent performance (Supplementary Figure S2). GENERanno matched Evo2-7B performance despite having 14-fold fewer parameters and using 12-fold less pretraining data, potentially due to its curated pretraining on actively expressed regions of the genome [18],

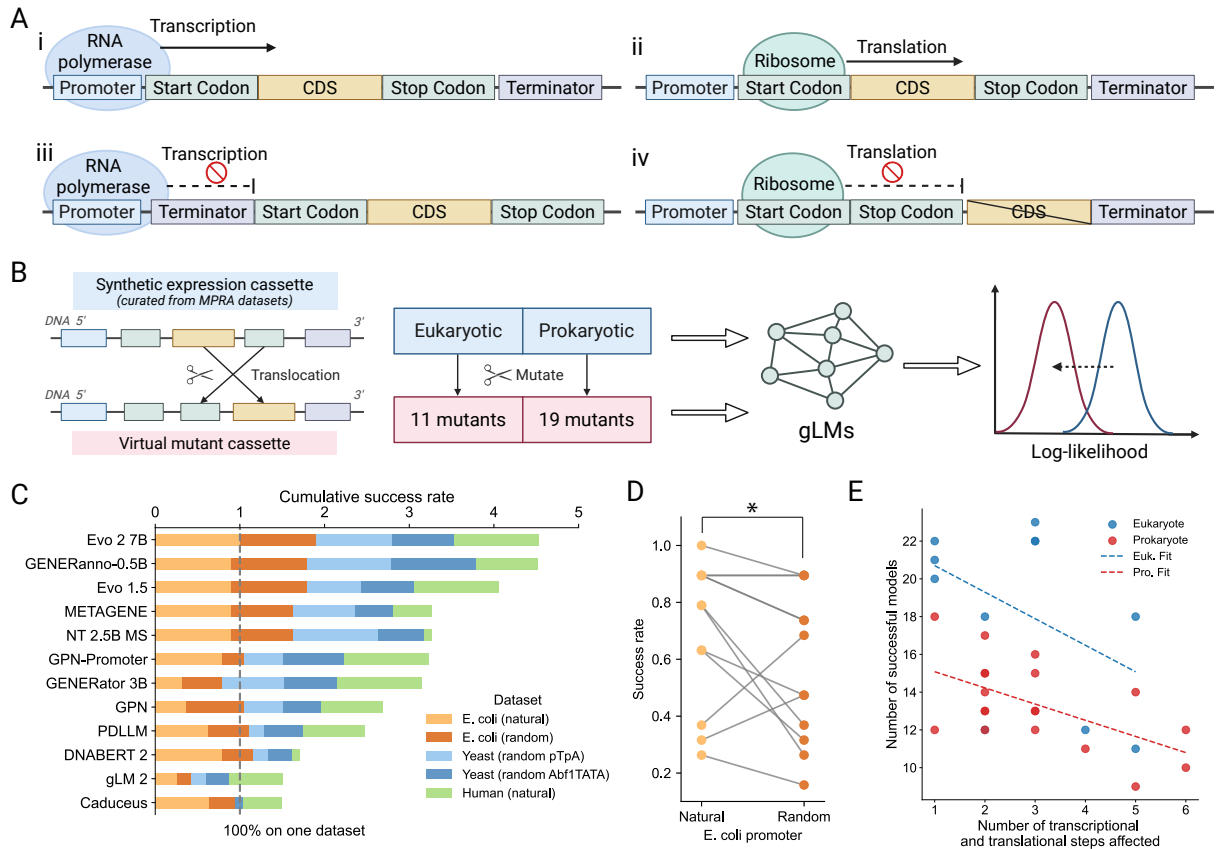


Figure 1: Overview of Nullsettes. A) Schematic examples showing transcription (i) and translation (ii) becoming impaired when the order of control element such as terminator (iii) or stop codon (iv) are altered. B) Nullsettes consist of 11 and 19 mutant variants for each eukaryotic and prokaryotic expression cassette, respectively, by translocating control elements, and evaluates how well gLMs can predict these loss-of-function mutations based on changes in log-likelihood. We curate functional nonmutant cassettes from five MPRA datasets. C) Cumulative success rates of representative gLMs evaluated on five MPRA datasets, with promoter either being random sequences or based on natural promoter (indicated in bracket). The two yeast datasets use promoter containing both natural motifs (Abf1-TATA, polyT-polyA) and random sequences. Dashed lines denote 100% success on one dataset. Models are sorted by cumulative success rate. D) Success rates of models in identifying Nullsettes mutants for *E. coli* expression cassettes with either naturally-derived or random promoters. Each line connects the performance of a single model across the two sets of cassettes. Statistical significance with $p < 0.05$ for a one-sided paired T-test. E) Scatter plot depicting the relationship between the number of transcriptional and translational steps affected (x-axis) and the number of models that successfully assign low pseudo-likelihood (y-axis) across Nullsettes mutants. Each point represents a distinct type of Nullsettes mutant, with eukaryotic ($n = 11$) and prokaryotic ($n = 19$) variants shown in blue and red, respectively. Dashed lines indicate linear regression fits for each group.

suggesting that data quality and relevance may matter more than scale for functional generalization. Supporting this hypothesis, performance did not consistently improve with scaling across four model families (Supplemental Figure S3).

Current gLMs recognize what natural expression cassettes look like, but not how they work, failing to generalize to contexts that deviate strongly from natural sequence statistics. Across most models, performance drops significantly when identifying mutants with strong

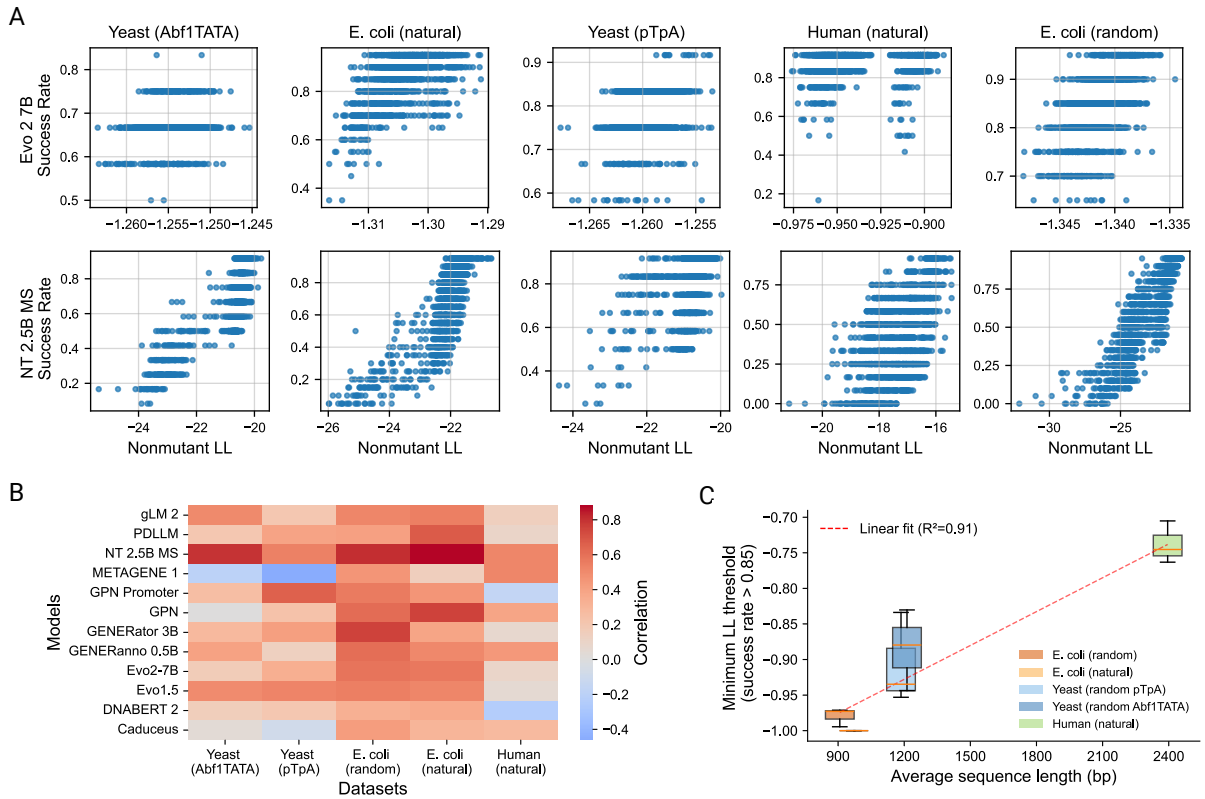


Figure 2: Relationship between gLM likelihood and zero-shot performance on mutation effect prediction. A) Each point represents an expression cassette. Scatterplots show the Nullsettes prediction performance of Evo2-7B and NT-2.5B-MS for cassettes from five datasets. B) Heatmap showing correlation between the gLM log likelihood (LL) of a sequence and gLM success rate on predicting its corresponding Nullsettes, across five datasets and 12 models. C) Log-likelihood (LL) threshold to achieve a success rate > 0.85 across datasets of increasing sequence length. Boxplots show the distribution of LL thresholds for top performing models (GENERanno, Evo2-7B, and Evo1.5) across five datasets, rescaled by lowest threshold. Datasets are ordered according to their average sequence length. Red dashed line is linear regression fit to the median threshold for each dataset.

promoters drawn from random sequence libraries compared to promoters derived from nature ($p = 0.04$)(Figure 1D). When evolutionary plausibility is not a useful prior for function, as these random sequences are assigned significantly lower LL (Supplementary Figure S1), models struggle to predict mutation effects.

A similar failure emerges across Nullsette mutations, with model performance worsening as mutations disrupt more steps of the gene expression process (Figure 1E). If models understood how genetic elements mechanistically drive expression, their predictions should remain robust or even improve as mutations become more disruptive. Instead, performance declines, suggesting that models do not reason about functional mechanism, and behave sensibly only within the distribution of natural sequences. We quantify disruption by counting the transcribed and translated elements missing in each mutant. When only one step is affected (e.g., a premature stop codon), the mutant remains close to natural sequence space, and models can often detect the resulting loss of function. But when multiple steps are disrupted (e.g., loss of both transcription and translation), the sequence falls further outside the distribution seen during training, and

model outputs become unreliable. Taken together, these results show that current gLMs do not understand regulatory logic, generalizing based on sequence similarity to evolutionary prior.

Across all gLMs, zero-shot performance in mutation effect prediction declines sharply as the log-likelihood (LL) of the original (nonmutant) sequence decreases, reinforcing that models rely on their evolutionary priors rather than a mechanistic understanding of DNA function. If a model understood how mutations disrupt gene expression, its predictions should depend on what function the mutation alters, not on how similar the sequence looks to the model’s training corpus. In that case, LOF mutants would be correctly identified regardless of the LL of the nonmutant cassette. However, we do observe this dependency on LL. Figure 2A shows this relationship for Evo2-7B and NT-2.5B-MS. For both models, the ability to detect LOF mutations improves consistently as the LL of the nonmutant increases. For example, in the *E. coli* (random) dataset [14], NT-2.5B-MS fails almost completely when $LL < -27$, but performs well above 80% when $LL > -22$. This dependency is not specific to a single model. As shown in Figure 2B, the same correlation between nonmutant LL and prediction accuracy holds across nearly all models, regardless of architecture or training corpus, indicating a shared reliance on sequence prior rather than reasoning about expression mechanisms.

Among top-performing models, the threshold LL required for high prediction accuracy is consistent and scales linearly with sequence length. Figure 2A shows that the minimum LL threshold for accurate prediction can vary widely across datasets. For example, NT-2.5B-MS achieves a success rate of 0.85 at a threshold LL of approximately -20 for Yeast (Abf1TATA) cassettes, but around -16 for Human (natural). For each model–dataset pair, we estimate the LL threshold corresponding to a success rate of 0.85 using linear regression. Figure 2C reveals that these thresholds are consistent among top performing models (after rescaling by lowest threshold). Furthermore, this threshold scales linearly with sequence length, showing a simple linear model can predict an effective LL threshold for zero-shot mutation effect prediction.

3 Conclusions

In this study, we introduce Nullsettes, a benchmark for evaluating the ability of genomic language models (gLMs) to understand DNA function by predicting loss-of-function (LOF) mutations in synthetic expression cassettes. Our analysis of 12 state-of-the-art models reveals that most struggle to consistently identify these LOF mutations, often relying on surface-level similarity rather than true functional understanding of regulatory elements. Reinforcing this fact, we show that LOF prediction accuracy declines sharply when nonmutant sequences have low gLM-assigned log-likelihood, as is the case for synthetic sequences. Comparing performance between models, we find a key avenue for improving functional understanding may be prioritizing curated, functionally relevant pretraining data over brute-force scaling. Together, these findings expose critical limitations in current gLMs and highlights the need for benchmark and modeling strategies that prioritize functional understanding for cell engineering.

4 Methods

4.1 Functional cassette curation

4.1.1 Prokaryote

To evaluate the regulatory grammar of prokaryotes on genomic language models, we utilized two benchmark datasets derived from synthetic expression constructs in *Escherichia coli*. The first, the Kosuri dataset [16], comprises combinatorial assemblies of promoters and ribosome binding sites (RBS) upstream of a superfolder GFP (sfGFP) reporter, designed to dissect transcriptional and translational contributions to gene expression. The second, the Lagator dataset [14], features a large-scale library of random promoter sequences with experimentally measured activity, enabling evaluation of models’ ability to generalize to highly diverse, out-of-distribution regulatory inputs.

4.1.2 Eukaryote

To evaluate the capacity of genomic language models to generalize to eukaryotic regulatory logic, we utilized two large-scale massively parallel reporter assay (MPRA) datasets. The Zahm dataset [17] comprises a library of 6,144 synthetic promoters constructed by combining transcriptional response elements (TREs) from 229 human and mouse transcription factors with minimal promoters. These constructs were assayed across multiple human cell lines and stimulatory conditions to quantify dynamic, stimulus-specific gene expression. The deBoer dataset [15] includes a comprehensive collection of 100 million randomized promoter sequences in yeast, enabling high-resolution dissection of cis-regulatory grammar under out-of-distribution scenario.

4.1.3 Promoter selection

To construct decoupled expression cassettes, we selected 1,500 promoters or promoter–RBS pairs from four distinct datasets.

For the Kosuri dataset [16], we selected candidate promoter–RBS pairs with protein expression levels exceeding $\mu + 1.5\sigma$ (10,165) across the full distribution. In contrast, given the limited number of highly active constructs in the Lagator dataset, we directly selected the top 1,500 promoter sequences ranked by protein output. We then compared the log-likelihood (LL) distributions of promoter–RBS groups using genomic language models including Evo1-8k, GENERator-3B, GPN, and NT-2.5B-MS. As the Lagator dataset [14] consists of randomly generated promoters, whereas the Kosuri library is more rationally designed, we prioritized Kosuri promoter–RBS pairs whose LL distributions surpassed those from Lagator (see Supplementary Figure S1A), yielding 1,500 expression cassettes from each dataset.

deBoer dataset [15] contains two promoter libraries: Abf1TATA and pTpA. Abf1TATA is designed by embedding conserved transcription factor binding sites such as Abf1 and a canonical TATA box, mimicking features of natural yeast promoters. In addition, pTpA consists of synthetic promoters constructed with a poly-T–poly-A architecture. Poly(dA–dT) sequences are naturally occurring motifs that associate with the centers of nucleosome-free regions in yeast promoters and serving as a hybrid natural + randomized library. We selectively constructed 1,500 active promoters for each dataset .

The Zahm dataset [17] comprises synthetic promoters built by coupling one of three minimal promoters—minCMV, minProm, or minTK—with diverse transcriptional response element (TRE) units. TRE units contain Transcription factor binding motifs (TFBMs) mostly derived from human genomes. To construct a representative set of mammalian expression cassettes, we selected the top 1,500 promoter-TRE combinations exhibiting the highest transcriptional activity.

4.2 Nullsettes Virtual Mutant Construction

To assess whether genomic language models can detect syntactic violations in gene regulatory architecture, we constructed Nullsettes—a benchmark of completely non-functional expression cassettes. These sequences were generated by systematic component translocations that disrupt the canonical transcription–translation structure while retaining all original components.

We first defined the canonical regulatory architecture for both prokaryote and eukaryote:

Prokaryotic systems (e.g., *E. coli*) contain six ordered elements: **Promoter - RBS - Start codon - CDS - Stop codon - Terminator**.

Eukaryotic systems (e.g., yeast, mammalian) consist of five ordered elements, lacking a RBS as translation initiation is guided by the 5' cap and the Kozak consensus sequence rather than a defined RBS: **Promoter - Start codon - CDS - Stop codon - Terminator**.

For each system, we generated all possible single-component translocation mutants, in which one element was relocated to a different position while preserving the identity and total count of elements.

To determine whether a mutant retained functional syntax, we evaluated each sequence against a minimal set of biologically grounded ordering constraints. These constraints ensure that proper CDS expression cannot be rescued by any flanking sequences outside the cassette. Specifically, we consider all circular permutations of each ordering and retain a mutant as a Nullsette only if no circular permutation of the mutant satisfies all three of the following rules:

Rule 1: Proper initiation ordering — Ensures that transcription starts upstream of translation initiation and that the CDS is translated from an upstream start codon.

Eukaryotic: $\text{Position(Promoter)} < \text{Position(Start codon)} < \text{Position(CDS)}$

Prokaryotic: $\text{Position(Promoter)} < \text{Position(RBS)} < \text{Position(Start codon)} < \text{Position(CDS)}$

Rule 2: Valid translation termination — The stop codon must follow the CDS or precede the start codon in circular order.

(i) $\text{Position(CDS)} < \text{Position(Stop codon)}$ or (ii) $\text{Position(Stop codon)} < \text{Position(Start codon)}$

Rule 3: Valid transcription termination — The terminator must lie downstream of the CDS or upstream of the promoter in circular form.

(i) $\text{Position(CDS)} < \text{Position(Terminator)}$ or (ii) $\text{Position(Terminator)} < \text{Position(Promoter)}$

After applying these rules across all circular permutations, we identified 19 non-functional translocation mutants in the prokaryotic system and 11 in the eukaryotic system, all of which violated the defined minimal functional syntax. These mutants are synthetically designed to be completely non-functional, challenging models to detect biologically catastrophic yet syntactically subtle disruptions in regulatory element ordering.

All mutant sequences are listed in Supplementary Table S1 (prokaryote) and Supplementary Table S2 (eukaryote).

4.3 Baseline Models

We benchmarked a diverse set of 12 self-supervised genomic foundation models that represent current state-of-the-art approaches to DNA language modeling. In general, the models can be categorized based on their tokenization schemes (fixed-length k-mers, single-nucleotide tokens, byte-pair encoding, and hybrid schemes), pretraining strategies (masked language modeling [19] vs. autoregressive modeling [20]), training corpus diversity (human references, plant genomes, multispecies genomes, and large-scale metagenomic assemblies), and architectural paradigms (CNN-based models, Transformer-based models [2], and emerging architectures like Striped-Hyena [21, 22] and Mamba [23]). Detailed model specifications are concluded in Supplementary Table S4 for casual language modeling-based models and S5 for mask language modeling-based models.

4.4 Evaluation Metrics

We computed the mean base-pair log-likelihood (LL) as the sequence-level LL score. To account for the distinct pretraining objectives of causal language models and masked language models, we applied different LL computation strategies.

Specifically, for casual language models (CLM), the log-likelihood of a nucleic acid sequence $X = (x_1, x_2, \dots, x_n)$ is computed using logits output from the model. Since CLM operates in an autogressive manner, each token x_t is predicted based on all previous token $x < t$. Given the model’s *logits* _{t} at each position t , the probability of the ground-truth token is obtained via softmax:

$$P(x_t | x_{<t}) = \frac{\exp(\text{logits}_{t,x_t})}{\sum_{v \in V} \exp(\text{logits}_{t,v})} \quad (1)$$

where V represents the vocabulary. The mean log-likelihood is then computed as:

$$\text{LL}_{\text{CLM}}(X) = \frac{1}{n-1} \sum_{t=2}^n \log P(x_t | x_{<t}) \quad (2)$$

Masked language models (MLMs) differ from autoregressive models in their inference behavior, as they are not inherently designed for sequential generation. To address this, Wang and Cho [24] introduced the pseudo log-likelihood (PLL) approach, wherein each token in a sequence is masked individually to compute token-wise conditional probabilities. More recently, Gordon et al. [25] proposed Single-Inference Pseudo Log-Likelihood, an efficient approximation that enables linear-time inference for BERT-style MLMs by exploiting training-time masking dynamics.

Rather than computing pseudo log-likelihood (PLL), we assessed relative changes in mean token-wise log-probabilities derived from unmasked logits for all MLM-based gLMs. This method, though lacking strict probabilistic interpretation, provides a scalable and effective proxy for quantifying model sensitivity to syntactic or functional disruptions. The formula is as follows:

Given the logits_t at each position t , the probability of the correct token is computed as:

$$P(x_t | X) = \frac{\exp(\text{logits}_{t,x_t})}{\sum_{v \in V} \exp(\text{logits}_{t,v})} \quad (3)$$

Then the log-likelihood for the entire sequence is computed over all positions:

$$\text{LL}_{\text{MLM}}(X) = \frac{1}{n} \sum_{t=1}^n \log P(x_t | X) \quad (4)$$

where all positions contribute to the likelihood computation since no masking is performed during inference.

To assess significance between paired conditions (e.g., original vs. mutant), we performed as one-sided paired permutation test. Given differences $d_i = x_i^{\text{mutant}} - x_i^{\text{original}}$ for each pair i , we computed the observed mean \bar{d}_{obs} . Under the null hypothesis of no effect, signs of d_i are exchangeable. We generated $N = 10,000$ random permutations by sampling $s_i \in \{-1, 1\}$ and computing $\bar{d}^{(j)} = \frac{1}{n} \sum_{i=1}^n s_i d_i$. The one-sided p-value was calculated as:

$$p = \frac{1}{N} \sum_{j=1}^N \mathbb{I}(\bar{d}^{(j)} \leq \bar{d}_{\text{obs}}) \quad (5)$$

for the alternative hypothesis that the mutant is smaller than the original.

5 Data availability

The expression cassette of Kosuri dataset [16] was obtained from <https://www.addgene.org/47441/>. The Lagator dataset [14] was downloaded from <https://github.com/szarma/Thermoters>. The deBoer dataset [15] was downloaded from <https://www.ncbi.nlm.nih.gov/geo/query/acc.cgi?acc=GSE104878>. The Zahm dataset [17] was downloaded from <https://www.ncbi.nlm.nih.gov/geo/query/acc.cgi?acc=GSE271608>.

6 Code availability

The source code for benchmarking gLMs and the Nullsettes used in this work is publicly available at: <https://github.com/cellethology/GLM-Nullsette-Benchmark>.

7 Acknowledgements

The authors thank members of the Cell Ethology Lab for valuable comments and suggestions. This work was supported by the Westlake Fellows Program at Westlake University.

8 Author Contributions

Z.J.W. conceived the initial proposal. S.J. and Z.J.W. jointly developed the overall concept and contributed to the framework design. S.J. implemented the framework. S.J., X.L., and Z.J.W.

conducted and analyzed the computational experiments. S.J. and Z.J.W. wrote the initial draft of the manuscript.

9 Competing interests

The authors declare no competing interests.

References

- [1] Gonzalo Benegas, Chengzhong Ye, Carlos Albors, Jianan Canal Li, and Yun S Song. Genomic language models: opportunities and challenges. *Trends in Genetics*, 2025.
- [2] Micaela E Consens, Cameron Dufault, Michael Wainberg, Duncan Forster, Mehran Karimzadeh, Hani Goodarzi, Fabian J Theis, Alan Moses, and Bo Wang. Transformers and genome language models. *Nature Machine Intelligence*, pages 1–17, 2025.
- [3] Brian L Hie, Varun R Shanker, Duo Xu, Theodora UJ Bruun, Payton A Weidenbacher, Shaogeng Tang, Wesley Wu, John E Pak, and Peter S Kim. Efficient evolution of human antibodies from general protein language models. *Nature biotechnology*, 42(2):275–283, 2024.
- [4] Yan He, Xibin Zhou, Chong Chang, Ge Chen, Weikuan Liu, Geng Li, Xiaoqi Fan, Mingsun Sun, Chensi Miao, Qianyue Huang, et al. Protein language models-assisted optimization of a uracil-n-glycosylase variant enables programmable t-to-g and t-to-c base editing. *Molecular Cell*, 84(7):1257–1270, 2024.
- [5] Qiang Zhang, Wanyi Chen, Ming Qin, Yuhao Wang, Zhongji Pu, Keyan Ding, Yuyue Liu, Qunfeng Zhang, Dongfang Li, Xinjia Li, et al. Integrating protein language models and automatic biofoundry for enhanced protein evolution. *Nature Communications*, 16(1):1553, 2025.
- [6] Jin Su, Zhikai Li, Chenchen Han, Yuyang Zhou, Yan He, Junjie Shan, Xibin Zhou, Xing Chang, Shiyu Jiang, Dacheng Ma, et al. Saprothub: Making protein modeling accessible to all biologists. *BioRxiv*, pages 2024–05, 2024.
- [7] Pascal Notin, Aaron Kollasch, Daniel Ritter, Lood Van Niekerk, Steffanie Paul, Han Spinner, Nathan Rollins, Ada Shaw, Rose Orenbuch, Ruben Weitzman, et al. Proteingym: Large-scale benchmarks for protein fitness prediction and design. *Advances in Neural Information Processing Systems*, 36:64331–64379, 2023.
- [8] Gonzalo Benegas, Sanjit Singh Batra, and Yun S Song. Dna language models are powerful predictors of genome-wide variant effects. *Proceedings of the National Academy of Sciences*, 120(44):e2311219120, 2023.
- [9] Yanyi Chu, Dan Yu, Yupeng Li, Kaixuan Huang, Yue Shen, Le Cong, Jason Zhang, and Mengdi Wang. A 5' utr language model for decoding untranslated regions of mrna and function predictions. *Nature Machine Intelligence*, 6(4):449–460, 2024.
- [10] Ziqi Tang, Nirali Somia, Yiyang Yu, and Peter K Koo. Evaluating the representational power of pre-trained dna language models for regulatory genomics. *Genome Biology*, 26(1):203, 2025.

- [11] Michael R Schlabach, Jimmy K Hu, Mamie Li, and Stephen J Elledge. Synthetic design of strong promoters. Proceedings of the national academy of sciences, 107(6):2538–2543, 2010.
- [12] Rongrong Du, Michael J Flynn, Monique Honsa, Ralf Jungmann, and Michael B Elowitz. miRNA circuit modules for precise, tunable control of gene expression. BioRxiv, 2024.
- [13] Xu Yan, Xu Liu, Cuihuan Zhao, and Guo-Qiang Chen. Applications of synthetic biology in medical and pharmaceutical fields. Signal transduction and targeted therapy, 8(1):199, 2023.
- [14] Mato Lagator, Srdjan Sarikas, Magdalena Steinrueck, David Toledo-Aparicio, Jonathan P Bollback, Calin C Guet, and Gašper Tkačik. Predicting bacterial promoter function and evolution from random sequences. Elife, 11:e64543, 2022.
- [15] Carl G de Boer, Eeshit Dhaval Vaishnav, Ronen Sadeh, Esteban Luis Abeyta, Nir Friedman, and Aviv Regev. Deciphering eukaryotic gene-regulatory logic with 100 million random promoters. Nature biotechnology, 38(1):56–65, 2020.
- [16] Sriram Kosuri, Daniel B Goodman, Guillaume Cambray, Vivek K Mutalik, Yuan Gao, Adam P Arkin, Drew Endy, and George M Church. Composability of regulatory sequences controlling transcription and translation in escherichia coli. Proceedings of the National Academy of Sciences, 110(34):14024–14029, 2013.
- [17] Adam M Zahm, William S Owens, Samuel R Himes, Braden S Fallon, Kathleen E Rondem, Alexa N Gormick, Joshua S Bloom, Sriram Kosuri, Henry Chan, and Justin G English. A massively parallel reporter assay library to screen short synthetic promoters in mammalian cells. Nature Communications, 15(1):10353, 2024.
- [18] Qiuyi Li, Wei Wu, Yiheng Zhu, Fuli Feng, Jieping Ye, and Zheng Wang. Generanno: A genomic foundation model for metagenomic annotation. bioRxiv, pages 2025–06, 2025.
- [19] Jacob Devlin, Ming-Wei Chang, Kenton Lee, and Kristina Toutanova. Bert: Pre-training of deep bidirectional transformers for language understanding. In Proceedings of the 2019 conference of the North American chapter of the association for computational linguistics: human language technologies, volume 1 (long and short papers), pages 4171–4186, 2019.
- [20] Tom Brown, Benjamin Mann, Nick Ryder, Melanie Subbiah, Jared D Kaplan, Prafulla Dhariwal, Arvind Neelakantan, Pranav Shyam, Girish Sastry, Amanda Askell, et al. Language models are few-shot learners. Advances in neural information processing systems, 33:1877–1901, 2020.
- [21] Michael Poli, Jue Wang, Stefano Massaroli, Jeffrey Quesnelle, Ryan Carlow, Eric Nguyen, and Armin Thomas. StripedHyena: Moving Beyond Transformers with Hybrid Signal Processing Models, 12 2023. URL <https://github.com/togethercomputer/stripedhyena>.
- [22] Jerome Ku, Eric Nguyen, David W Romero, Garyk Bixi, Brandon Yang, Anton Vorontsov, Ali Taghibakhshi, Amy X Lu, Dave P Burke, Greg Brockman, et al. Systems and algorithms for convolutional multi-hybrid language models at scale. arXiv preprint arXiv:2503.01868, 2025.
- [23] Albert Gu and Tri Dao. Mamba: Linear-time sequence modeling with selective state spaces. arXiv preprint arXiv:2312.00752, 2023.
- [24] Alex Wang and Kyunghyun Cho. Bert has a mouth, and it must speak: Bert as a markov random field language model. arXiv preprint arXiv:1902.04094, 2019.

- [25] Cade Gordon, Amy X Lu, and Pieter Abbeel. Protein language model fitness is a matter of preference. [bioRxiv](#), pages 2024–10, 2024.
- [26] Ollie Liu, Sami Jaghouar, Johannes Hagemann, Shangshang Wang, Jason Wiemels, Jeff Kaufman, and Willie Neiswanger. Metagene-1: Metagenomic foundation model for pandemic monitoring. [arXiv preprint arXiv:2501.02045](#), 2025.
- [27] Hugo Dalla-Torre, Liam Gonzalez, Javier Mendoza-Revilla, Nicolas Lopez Carranza, Adam Henryk Grzywaczewski, Francesco Oteri, Christian Dallago, Evan Trop, Bernardo P de Almeida, Hassan Sirelkhatim, et al. Nucleotide transformer: building and evaluating robust foundation models for human genomics. [Nature Methods](#), pages 1–11, 2024.
- [28] Wei Wu, Qiuyi Li, Mingyang Li, Kun Fu, Fuli Feng, Jieping Ye, Hui Xiong, and Zheng Wang. Generator: A long-context generative genomic foundation model. [arXiv preprint arXiv:2502.07272](#), 2025.
- [29] Eric Nguyen, Michael Poli, Matthew G Durrant, Brian Kang, Dhruva Katrekar, David B Li, Liam J Bartie, Armin W Thomas, Samuel H King, Garyk Bixi, et al. Sequence modeling and design from molecular to genome scale with evo. [Science](#), 386(6723):eado9336, 2024.
- [30] Aditi T Merchant, Samuel H King, Eric Nguyen, and Brian L Hie. Semantic mining of functional de novo genes from a genomic language model. [bioRxiv](#), pages 2024–12, 2024.
- [31] Garyk Bixi, Matthew G Durrant, Jerome Ku, Michael Poli, Greg Brockman, Daniel Chang, Gabriel A Gonzalez, Samuel H King, David B Li, Aditi T Merchant, et al. Genome modeling and design across all domains of life with evo 2. [bioRxiv](#), pages 2025–02, 2025.
- [32] Zhihan Zhou, Yanrong Ji, Weijian Li, Pratik Dutta, Ramana Davuluri, and Han Liu. Dnabert-2: Efficient foundation model and benchmark for multi-species genome. [arXiv preprint arXiv:2306.15006](#), 2023.
- [33] Yair Schiff, Chia-Hsiang Kao, Aaron Gokaslan, Tri Dao, Albert Gu, and Volodymyr Kuleshov. Caduceus: Bi-directional equivariant long-range dna sequence modeling. [arXiv preprint arXiv:2403.03234](#), 2024.
- [34] Gonzalo Benegas, Gökçen Eraslan, and Yun S Song. Benchmarking dna sequence models for causal regulatory variant prediction in human genetics. [bioRxiv](#), pages 2025–02, 2025.
- [35] Andre Cornman, Jacob West-Roberts, Antonio Pedro Camargo, Simon Roux, Martin Baracochea, Milot Mirdita, Sergey Ovchinnikov, and Yunha Hwang. The omg dataset: An open metagenomic corpus for mixed-modality genomic language modeling. [bioRxiv](#), pages 2024–08, 2024.
- [36] Guanqing Liu, Long Chen, Yuechao Wu, Yangshuo Han, Yu Bao, and Tao Zhang. Pdllms: A group of tailored dna large language models for analyzing plant genomes. [Molecular Plant](#), 18(2):175–178, 2025.

Supplementary Information

Supplemental Figures

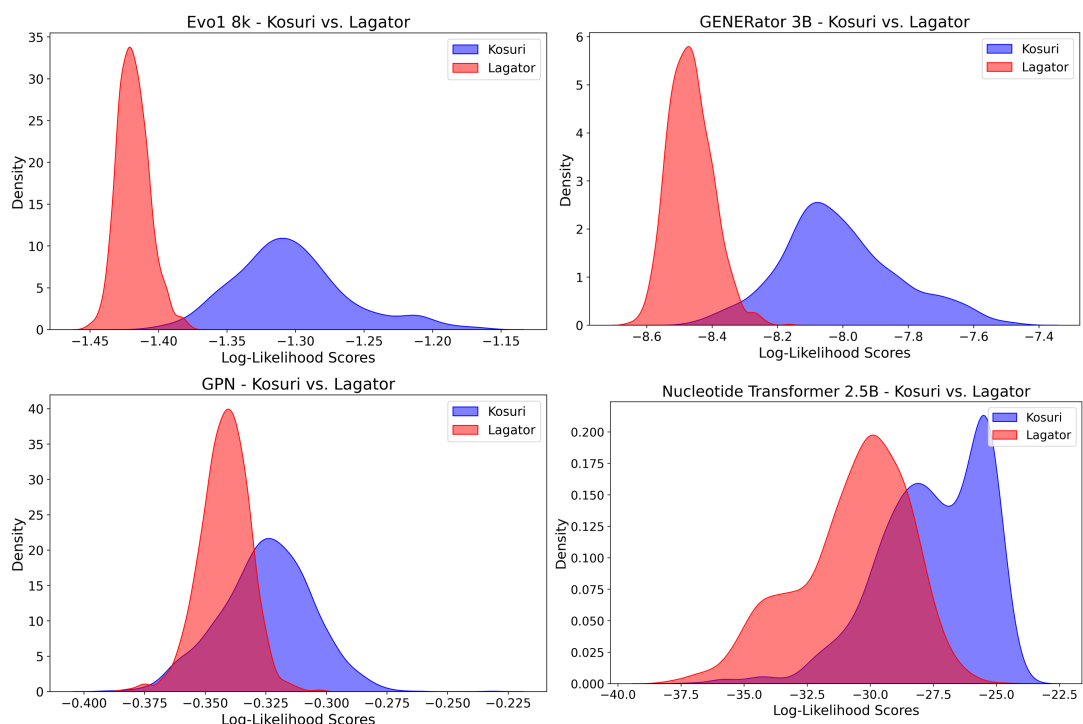


Figure S1: Comparison of promoter log-likelihood distribution

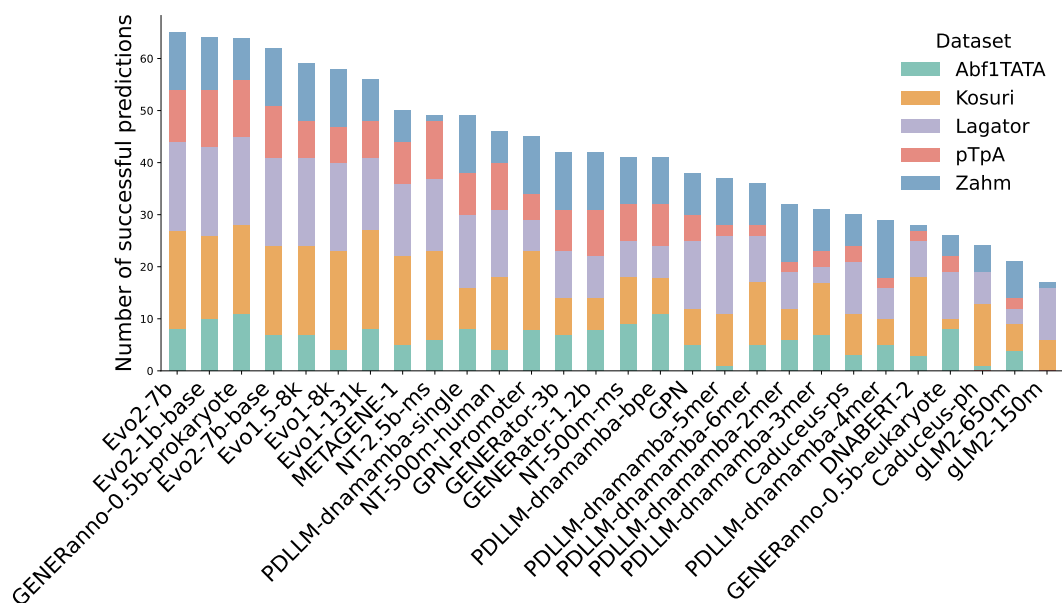


Figure S2: The number of cumulative successful predictions made by each model series across four datasets: Abf1TATA and pTpA (from deBoer), Zahm, Kosuri, and Lagator.

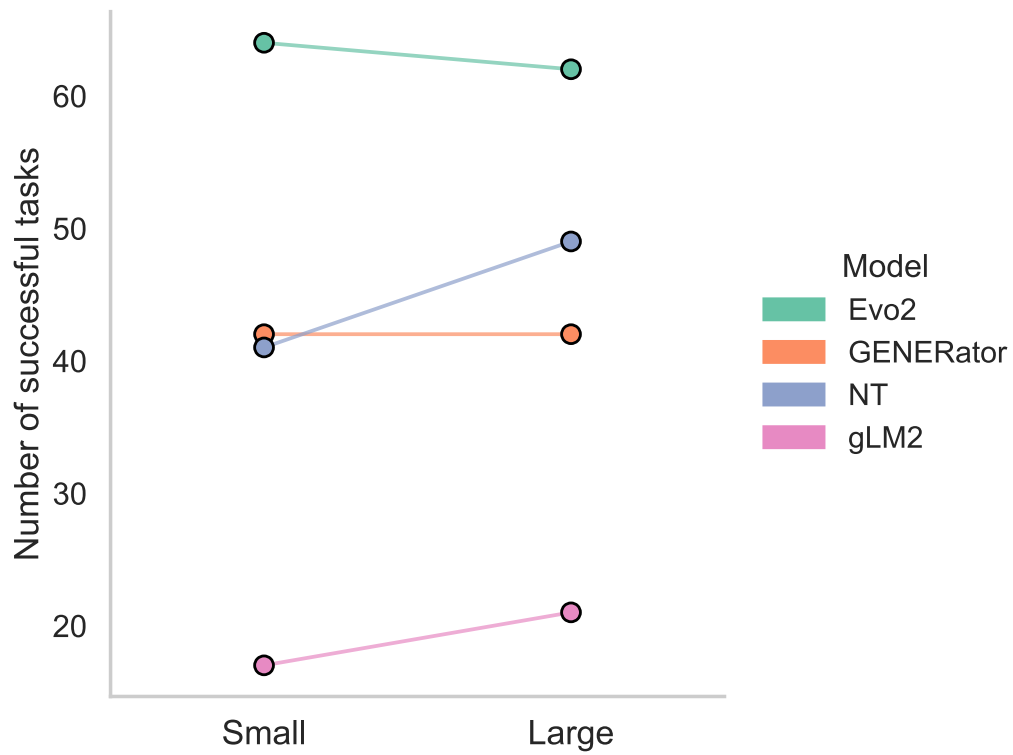


Figure S3: Number of Nullsette mutations successfully identified for gLMs with small and large variants, including Evo2 (1B vs. 7B), GENERator (1.2B vs. 3B), NT (500M vs. 2.5B, multispecies), and gLM2 (150M vs. 650M).

Supplemental Tables

Mutant ID	Description
Translocation-1	CDS - Promoter - RBS - Start codon - Stop codon - Terminator
Translocation-2	Promoter - CDS - RBS - Start codon - Stop codon - Terminator
Translocation-3	Promoter - RBS - CDS - Start codon - Stop codon - Terminator
Translocation-4	Promoter - RBS - CDS - Stop codon - Start codon - Terminator
Translocation-5	Promoter - RBS - CDS - Stop codon - Terminator - Start codon
Translocation-6	Promoter - RBS - Start codon - Stop codon - CDS - Terminator
Translocation-7	Promoter - RBS - Start codon - Stop codon - Terminator - CDS
Translocation-8	Promoter - RBS - Start codon - Terminator - CDS - Stop codon
Translocation-9	Promoter - RBS - Terminator - Start codon - CDS - Stop codon
Translocation-10	Promoter - Start codon - CDS - RBS - Stop codon - Terminator
Translocation-11	Promoter - Start codon - CDS - Stop codon - RBS - Terminator
Translocation-12	Promoter - Start codon - CDS - Stop codon - Terminator - RBS
Translocation-13	Promoter - Start codon - RBS - CDS - Stop codon - Terminator
Translocation-14	Promoter - Terminator - RBS - Start codon - CDS - Stop codon
Translocation-15	RBS - Promoter - Start codon - CDS - Stop codon - Terminator
Translocation-16	RBS - Start codon - CDS - Promoter - Stop codon - Terminator
Translocation-17	RBS - Start codon - CDS - Stop codon - Promoter - Terminator
Translocation-18	RBS - Start codon - Promoter - CDS - Stop codon - Terminator
Translocation-19	Start codon - Promoter - RBS - CDS - Stop codon - Terminator

Table S1: **Prokaryotic virtual mutant cases.** Translocation-3,4,5 cannot be compensated by a later start codon as there are no other in-frame start codon.

Mutant ID	Description
Translocation-1	CDS - Promoter - Start codon - Stop codon - Terminator
Translocation-2	Promoter - CDS - Start codon - Stop codon - Terminator
Translocation-3	Promoter - CDS - Stop codon - Start codon - Terminator
Translocation-4	Promoter - CDS - Stop codon - Terminator - Start codon
Translocation-5	Promoter - Start codon - Stop codon - CDS - Terminator
Translocation-6	Promoter - Start codon - Stop codon - Terminator - CDS
Translocation-7	Promoter - Start codon - Terminator - CDS - Stop codon
Translocation-8	Promoter - Terminator - Start codon - CDS - Stop codon
Translocation-9	Start codon - CDS - Promoter - Stop codon - Terminator
Translocation-10	Start codon - CDS - Stop codon - Promoter - Terminator
Translocation-11	Start codon - Promoter - CDS - Stop codon - Terminator

Table S2: **Eukaryotic virtual mutant cases.** Translocation-2,3,4 cannot be compensated by a later start codon as there are no other in-frame start codon.

Model series	Representative variant
METAGENE1 [26]	METAGENE-1 (METAGENE1)
Nucleotide Transformer [27]	nucleotide-transformer-2.5b-multi-species (NT-2.5B-NT)
GENERator [28]	GENERator-eukaryote-3b-base (GENERator-3B)
GENERanno [18]	GENERanno-prokaryote-0.5b-base (GENERanno-0.5B)
Evo1 [29, 30]	evo-1.5-8k-base (Evo1.5)
Evo2 [31]	evo2_7b_base (Evo2-7B)
DNABERT2 [32]	DNABERT-2-117M (DNABERT2)
Caduceus [33]	caduceus-ph_seqlen-131k_d_model-256_n_layer-16 (Caduceus)
GPN [8]	gpn-brassicales (GPN)
GPN-Promoter [34]	gpn-animal-promoter (GPN-Promoter)
gLM2 [35]	gLM2_650M (gLM2)
PDLLM [36]	PDLLM-dnamamba-6mer (PDLLM)

Table S3: **Representative model variant.** For each model series, we list a representative variant used in major benchmarking. The official model identifier is listed, followed in parentheses by the shorthand name used throughout the main text. For example, the variant “nucleotide-transformer-2.5b-multi-species” is referred to as “NT-2.5B-NT” in the text.

Model name	Pretraining dataset	Pretraining method	Tokenization	Architecture	Input length
Evo1 8k [29]	OpenGenome: Prokaryotic whole-genomes dataset (300B tokens).	CLM	Single-nucleotide tokens	StripedHyena, 7B params	Pretrained with 8,192 context
Evo1 131k [29]	OpenGenome: Prokaryotic whole-genomes dataset (300B tokens).	CLM	Single-nucleotide tokens	StripedHyena, 7B params	Pretrained with 131,072 context using Evo1 8k as the base model
Evo1.5 [30]	50% increase in training data comparing to Evo1	CLM	Single-nucleotide tokens	StripedHyena, 7B params	Pretrained with 8,192 context using Evo1 8k as the base model
Evo2 1B base [31]	OpenGenome2: a dataset containing 8.8 trillion tokens from all domains of life.	CLM	Single-nucleotide tokens	StripedHyena 2, 1B params	Pretrained with 8192 context length
Evo2 7B base [31]	OpenGenome2: a dataset containing 8.8 trillion tokens from all domains of life.	CLM	Single-nucleotide tokens	StripedHyena 2, 7B params	Pretrained with 8192 context length
Evo2 7B [31]	OpenGenome2: a dataset containing 8.8 trillion tokens from all domains of life.	CLM	Single-nucleotide tokens	StripedHyena 2, 7B params	Pretrained with 1M context using Evo2 7b base as the base model
GENERator eukaryote 3B [28]	Eukaryotic genomes (386B bp), plants, fungi, protozoa, mammalian, vertebrate, invertebrate.	CLM	6-mer	Llama-based decoder, 3B params	Pretrained with a context length of 98k bp
GENERator eukaryote 1.2B [28]	Eukaryotic genomes (386B bp), plants, fungi, protozoa, mammalian, vertebrate, invertebrate.	CLM	6-mer	Llama-based decoder, 1.2B params	Pretrained with a context length of 98k bp
METAGEN-1 [26]	1.5T base pairs of DNA and RNA sequences from human wastewater samples.	CLM	Byte-pair encoding	Llama-2, 7B params	Pretrained with 512 sequence length
PDLLM-DNAMamba [36]	Plant reference genomes	CLM	6-mer/5-mer/4-mer/3-mer/2-mer/single/BPE	SSM, 130M params	Pretrained max token length is 512

Table S4: Casual language modeling (CLM) based genomic language models

Model name	Pretraining dataset	Pretraining method	Tokenization	Architecture	Input length
Nucleotide Transformer 2.5B multispecies [27]	850 whole genomes from NCBI, plants and viruses are not included, resulting in a total of 174B nucleotides, i.e. roughly 29B tokens.	MLM	6-mers	Transformer, 2.5B params	1000 bp
Nucleotide Transformer 500M multispecies [27]	850 whole genomes from NCBI, plants and viruses are not included, resulting in a total of 174B nucleotides, i.e. roughly 29B tokens.	MLM	6-mers	Transformer, 500M params	1000 bp
Nucleotide Transformer 500M Human ref [27]	GRCh38 human reference genome, resulting in 3B nucleotides, i.e. roughly 500M 6-mer tokens.	MLM	6-mers	Transformer, 500M params	1000 bp
GENERanno prokaryote 0.5B base [18]	715 billion base pairs of prokaryotic DNA	MLM	single-nucleotide	Transformer encoder, 500M params	8k bp
GENERanno eukaryote 0.5B base [18]	386 billion base pairs of eukaryotic DNA	MLM	single-nucleotide	Transformer encoder, 500M params	8k bp
Caduceus-ph [33]	Human reference genome (35M tokens / nucleotide base pairs).	MLM	Single-nucleotide tokens	BiMamba, 7.7M params	Pretrained with 131,072 sequence length (reverse complement augmentation)
Caduceus-ps [33]	Human reference genome (35M tokens / nucleotide base pairs).	MLM	Single-nucleotide tokens	BiMamba, 7.7M params	Pretrained with 131,072 sequence length (No reverse complement augmentation)
GPN [8]	Brassicales reference genome from NCBI Genome. Took the union of exons (with a small intronic flank), promoters (1,000 bp upstream of transcription start sites) as well as an equivalent amount of random windows from the whole genome.	MLM	Single-nucleotide tokens	CNN	512 bp
GPN-Promoter [34]	Animal promoter, genomes of 434 animal species.	MLM	Single-nucleotide tokens	ByteNet, 152M	Pretrained on 512 bp sequences centered at TSSs of protein-coding genes
DNABERT2 [32]	Human genome dataset (2.75B nucleotide bases) + Multispecies genome dataset (from 135 species, spread across 6 categories). The dataset includes 32.49B nucleotides bases, excluding all sequence with N and retain only ATCG.	MLM	Byte-pair encoding	BERT, 117M params	Pretrained on 700 bp length sequences
gLM2 [35]	OMG: encodes genomic scaffolds with both amino-acid (CDS) and DNA tokens (315B tokens).	MLM	Char-level tokens (DNA: lowercase, AA: uppercase)	Transformer, 650M params / 150M params	Pretrained with a 4096 token context window

Table S5: Mask language modeling (MLM) based genomic language models